Electronic Supplementary Material (ESI) for RSC Advances.
This journal is © The Royal Society of Chemistry 2022

# Supplement revised

# Eu- and Tb-adsorbed $Si_3N_4$ and $Ge_3N_4$: Tuning the colours with one luminescent host

Cordula Braun,[a]* Liuda Mereacre,[a] Zheng Chen,[b] Adam Slabon,[c]
David Vincent,[d] Xavier Rocquefelte,[d] and Jean-François Halet[e]

[a] * Dr. C. Braun, L. Mereacre,
Karlsruhe Institute of Technology (KIT)
Institute for Applied Materials
Herrmann-von-Helmholtz-Platz 1,
D-76344 Eggenstein-Leopoldshafen
E-mail: Cordula.Braun@kit.edu

[b] Z. Chen,
Institute of Inorganic Chemistry, RWTH Aachen University,
Landoltweg 1,
D-52056 Aachen

[c] Prof. Dr. A. Slabon,
Chair of Inorganic Chemistry,
University of Wuppertal
Gaussstr. 20
42119 Wuppertal, Germany

[d] D. Vincent, Prof. Dr. X. Rocquefelte,
Univ. Rennes - CNRS
Institut des Sciences Chimiques de Rennes, UMR 6226
35000 Rennes, France

[e] Prof. Dr. J.-F. Halet
CNRS – Saint-Gobain – NIMS, IRL 3629,
Laboratory for Innovative Key Materials and Structures (LINK),
National Institute for Materials Science (NIMS),
1-1 Namiki, Tsukuba 305-0044, Japan

***Figure(s)***

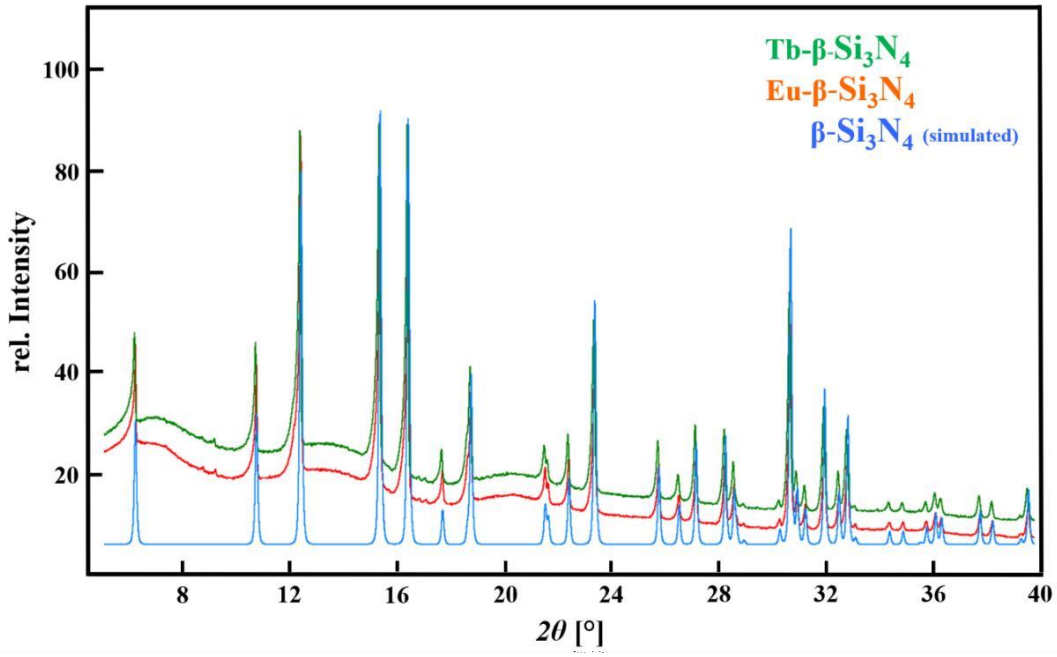


Figure S1: X-ray powder diffraction pattern of Eu-β-$Si_3N_4$ (red) and Tb-β-$Si_3N_4$ (green), β-$Si_3N_4$ simulated from ICSD 170006 (light blue), ($\lambda$ = 0.709026 Å).

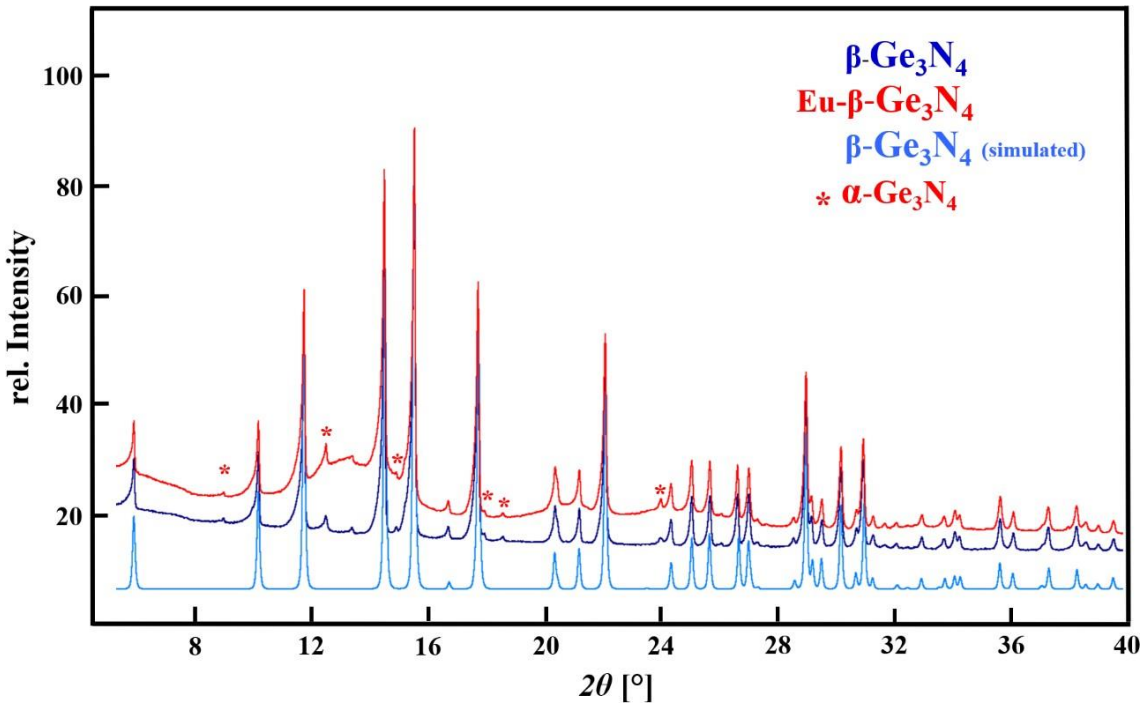


Figure S2: X-ray powder diffraction pattern of pure β-$Ge_3N_4$ (blue), Eu-β-$Ge_3N_4$ (red), β-$Ge_3N_4$ simulated from ICSD 658934 (light blue), * marks α-$Ge_3N_4$ ($\lambda$ = 0.709026 Å).

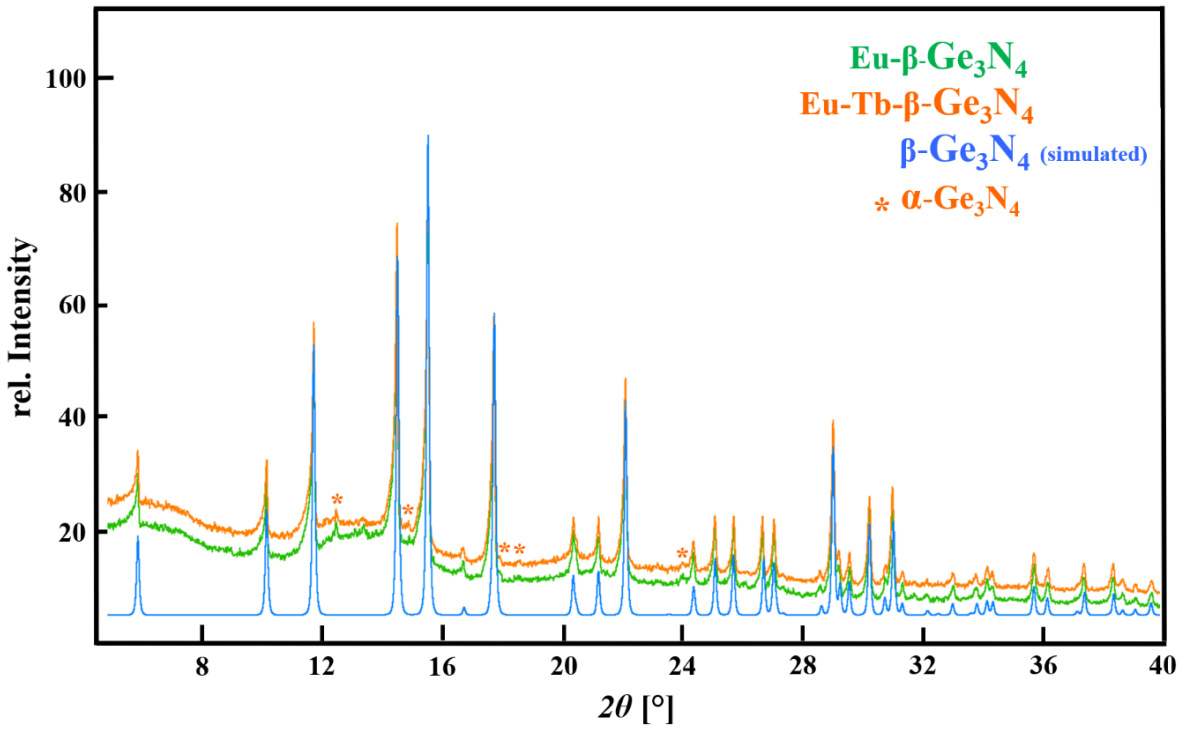


Figure S3: X-ray powder diffraction pattern of Tb-β-$Ge_3N_4$ (green), Eu,Tb-β-$Ge_3N_4$ (orange), β-$Ge_3N_4$ simulated from ICSD 658934 (light blue), * marks α-$Ge_3N_4$ ($\lambda$ = 0.709026 Å).

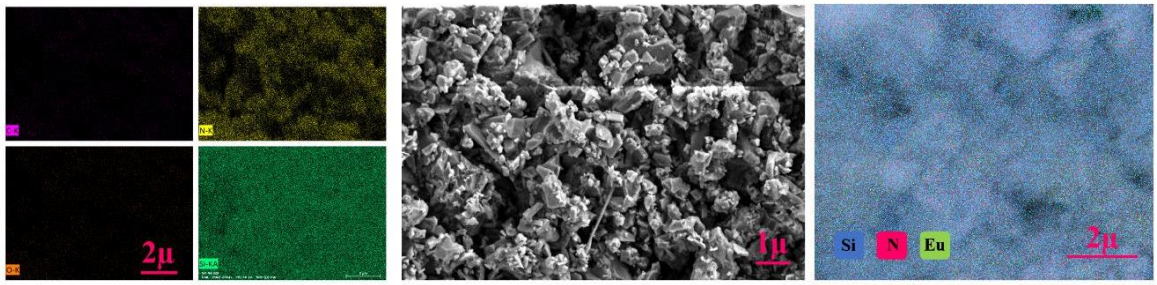


Figure S4: a) REM-EDX of pure β-$Si_3N_4$, b) SEM of pure β-$Si_3N_4$, c) REM-EDX of Eu-β-$Si_3N_4$ distribution of Si (blue), N (pink) and Eu (green).

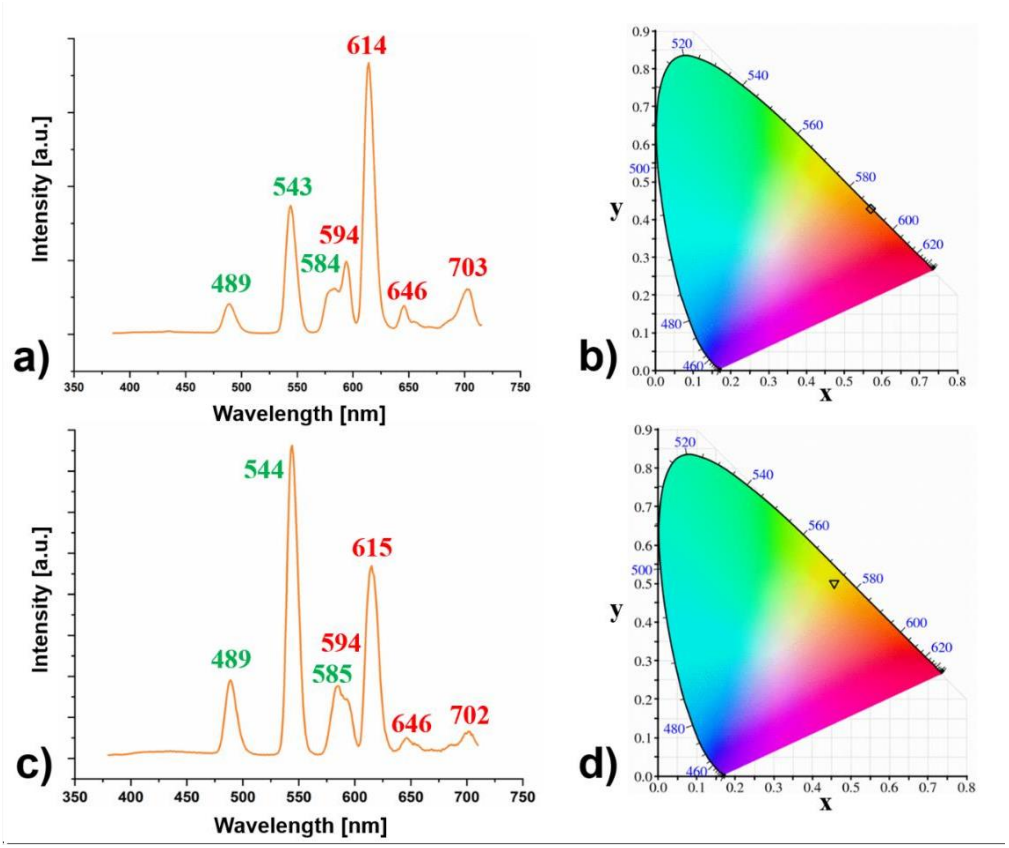


Figure S5: a) Luminescence spectrum of Eu-β-$Si_3N_4$ and Tb-β-$Si_3N_4$ powders mixed in a mortar, b) CIE diagram of Eu-$Si_3N_4$ and Tb-$Si_3N_4$ powders mixed in a mortar, c) Luminescence spectrum of Eu-$Ge_3N_4$ and Tb-$Ge_3N_4$ powders mixed in a mortar, d) CIE diagram of Eu-β-$Ge_3N_4$ and Tb-β-$Ge_3N_4$ powders mixed in a mortar.

***Comparison with literature***

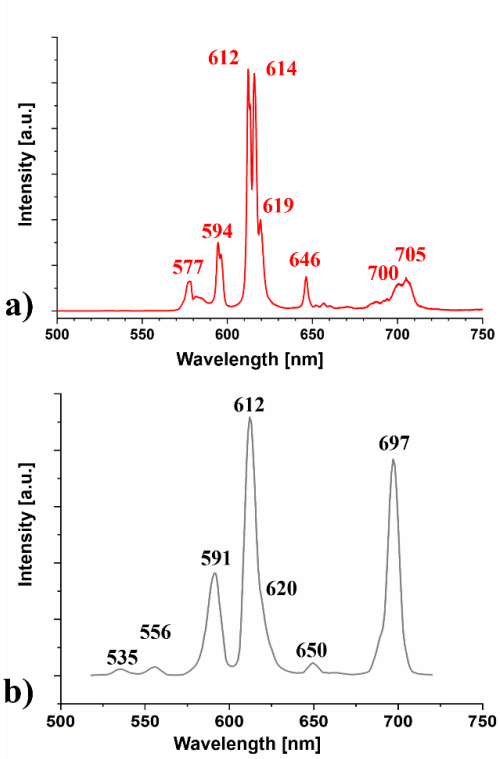


Figure S6: Luminescence spectra of a) Eu-β-$Si_3N_4$ and b) $EuCl_3$ *x* 6 $H_2O$.

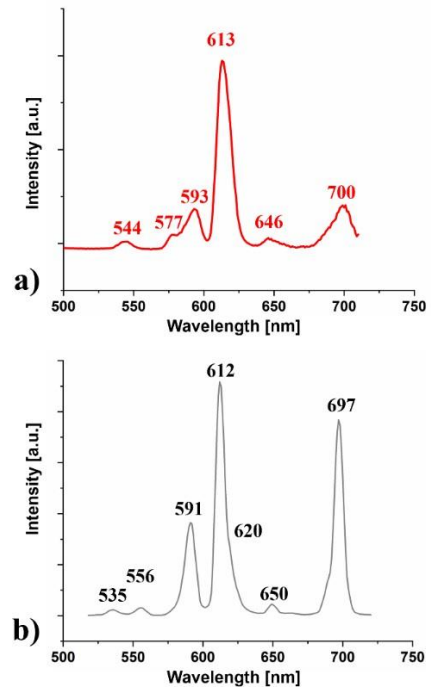


Figure S7: Luminescence spectra of a) Eu-β-$Ge_3N_4$ and b) $EuCl_3$ *x* 6 $H_2O$.

The works of Li *et al.*[1] deal with the photoluminescence properties of rare-earth doped nanocrystalline α-$Si_3N_4$. Here we use the expression doping explicitly as this is the title of the work of Li *et al.*[1] The doping has been done with Eu- and Tb-oxide and the authors confirm the oxygen content playing an important role. Furthermore, the content of the lanthanoids must not exceed 0.5 mol%, because otherwise α-$Si_3N_4$ was no longer stable. They describe the $Eu^{2+}$-doped α-$Si_3N_4$ to show a blue band emission peak at around 460 and 470 nm which is completely different to the red luminescence of $Eu^{3+}$ known from literature[2–4] When using EuN as a dopant the luminescence intensity decreases significantly. (see Figure S7) Regarding the doping of α-$Si_3N_4$ with $Tb_4O_7$ the result was declared as $Tb_{0.005}Si_{2.985}N_{3.964}O_{0.00875}$.[1] (See Figure S12)

Li *et al.*[5] describe a Eu-doped yellow phosphor consisting of a mixed phase of nanocrystalline α-$Si_3N_4$ and β-$Si_3N_4$. It was realized by reacting solid polycarbosilane with europium acetylacetonate hydrate and followed by nitridation and calcination of the precursor. The broad band luminescence peak is around 550 nm, resulting in a yellow greenish colour. The authors confirmed an oxygen as well as a carbon content resulting in the formation of nonstoichiometric $Si_3N_4$. (see Figure S8)

Yin *et al.*[6] synthesized very thin and wide single-crystal α-$Si_3N_4$ nanobelts by a vapor-solid thermal reaction featuring a very broad band emission spectrum 420-750 nm with a maximum at 575 nm. But here no doping with rare-earth ions is reported.

Su *et al.*[7] prepared ultra-long, single crystal, Eu-doped α-Si3N4 nanowires by nitriding Eu-doped cryomilled nanocrystalline Si powder resulting in a very broad band green emission around 570 nm. (see Figure S9)

Xu *et al.*[8] introduced $Eu^{2+}$-doped α-$Si_3N_4$ nanowires coated with a thin BN film. (see Figure S10) The relationship between photoluminescence and intrinsic point defects in α-$Si_3N_4$ via band structure modelling based on density functional theory calculations is interpretated by Huang *et al.*.[9] Huang *et al.*[10] present formation energies, electronic and optical properties of Y-doped $Si_3N_4$ on the basis of DFT calculations. Huang and coworkers[11] report the photoluminescence behavior of ultra-pure α-$Ge_3N_4$ nanowires resulting in a blue-green luminescence (440 nm) from the electronic transition from the conduction band to valence band. Huang *et al.*[12] report the doping of single-crystalline α-$Si_3N_4$ nanowires (Y, Ce, Tb) via directly nitriding-doped nanocrystalline silicon powders. A comparison of the luminescence spectra of these one-dimensional nanomaterials with doped bulk material Tb-β-$Si_3N_4$ (see Figure S13) indicates clear differences. Also the doping of α-$Si_3N_4$:Eu displays a completely divers broad band luminescence peak around 578 nm. (see Figure S11)

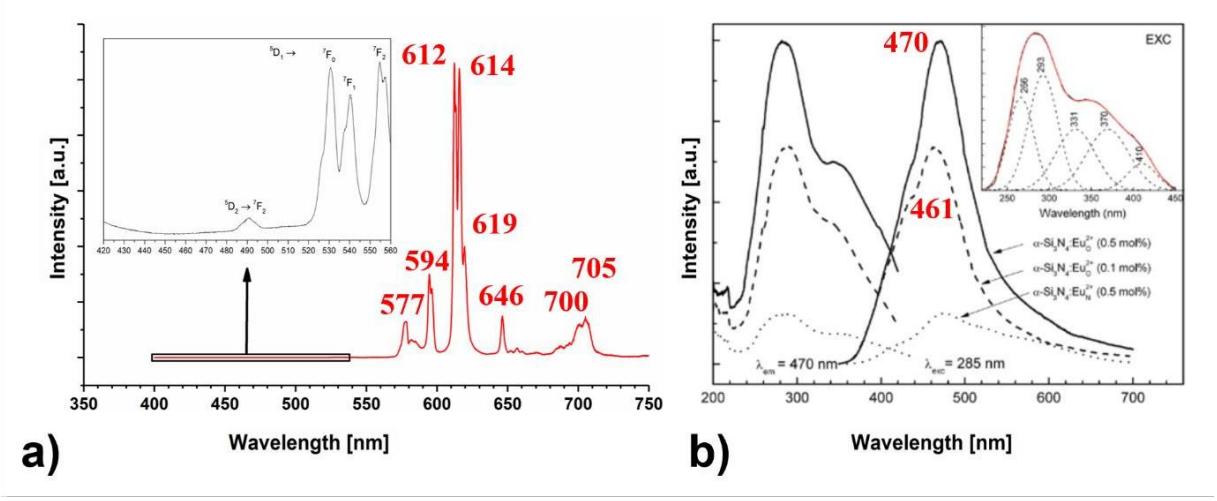


Figure S8: Luminescence spectra of a) Eu-β-$Si_3N_4$ and b) α-$Si_3N_4$:Eu.[1] (Wavelengths are estimated from the scale in *ref.*[1])

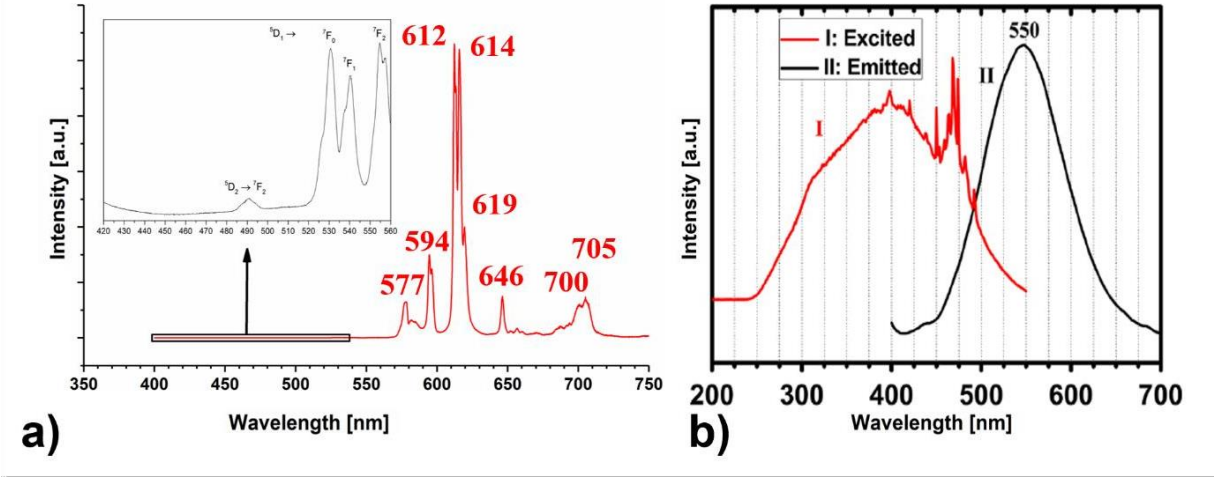


Figure S9: Luminescence spectra of a) Eu-β-$Si_3N_4$ and b) α-$Si_3N_4$:Eu.[5] (Wavelengths are estimated from the scale in *ref.*[5])

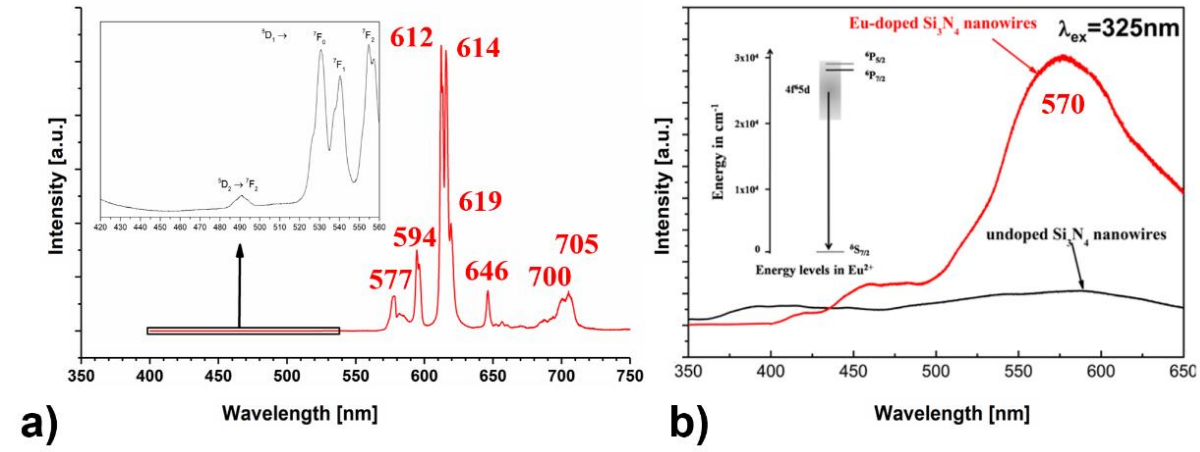


Figure S10: Luminescence spectra of a) Eu-β-$Si_3N_4$ and b) α-$Si_3N_4$:Eu.[7] (Wavelengths are estimated from the scale in *ref.*[7])

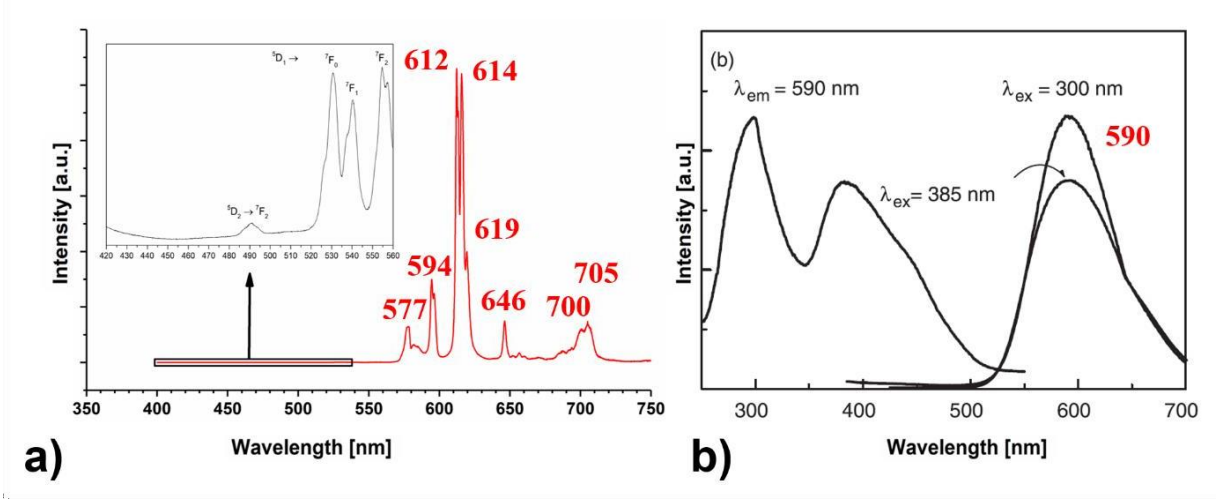


Figure S11: Luminescence spectra of a) Eu-β-$Si_3N_4$ and b) α-$Si_3N_4$:Eu nanowires coated with a thin BN film.[8] (Wavelengths are estimated from the scale in *ref.*[8])

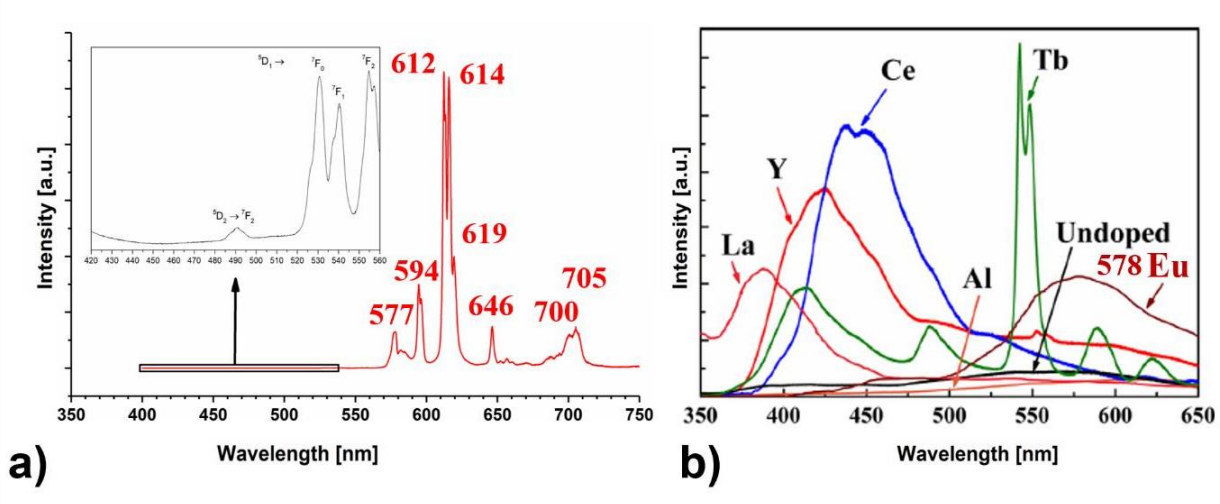


Figure S12: Luminescence spectra of a) Eu-β-$Si_3N_4$ and b) α-$Si_3N_4$:Eu nanowires.[12] (Wavelengths are estimated from the scale in *ref.*[12])

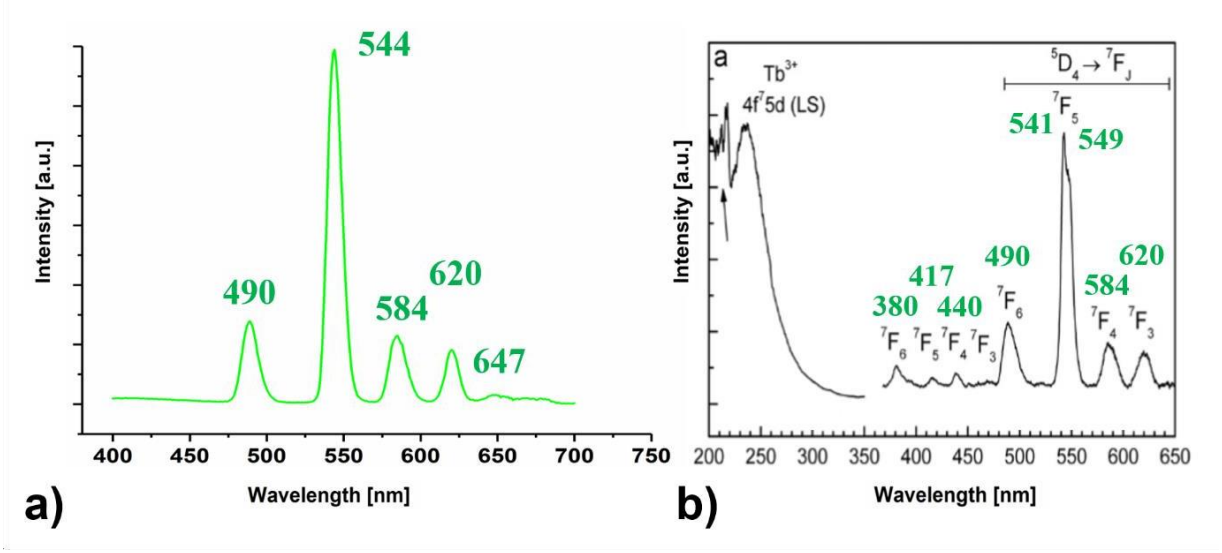


Figure S13: Luminescence spectra of a) Tb-β-$Si_3N_4$ and b) α-$Si_3N_4$:Tb[1] (Wavelengths are estimated from the scale in *ref.*[1])

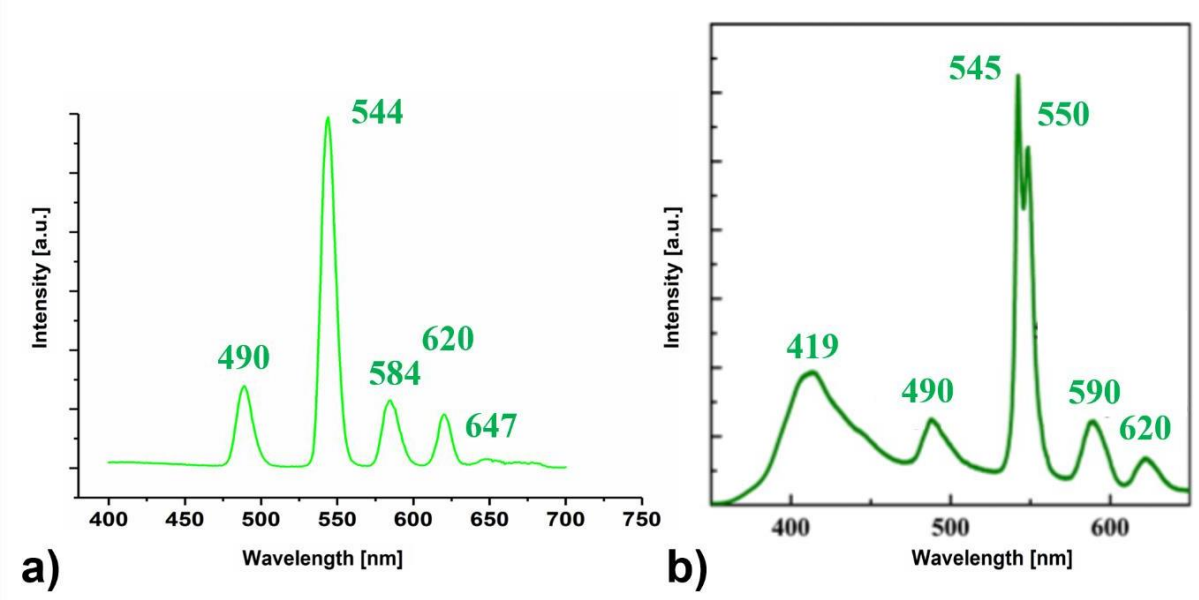


Figure S14: Luminescence spectra of a) $Si_3N_4$:Tb and b) $Si_3N_4$:Tb Nanowires[12] (Wavelengths are estimated from the scale in *ref.*[12])

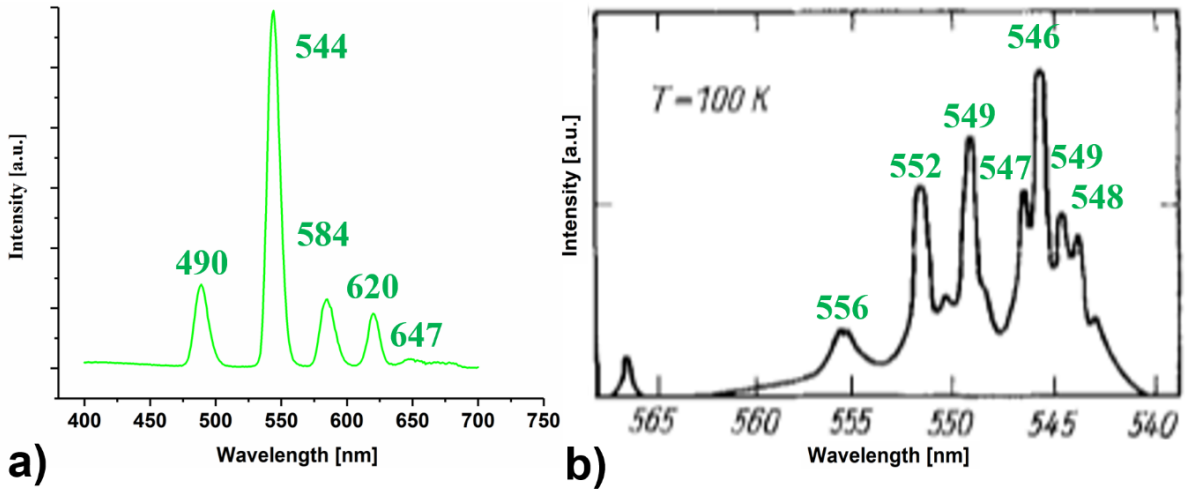


Figure S15: Luminescence spectra of a) $Si_3N_4$:Tb and b) TbOCl.[13] (Wavelengths are estimated from the scale in *ref.*[13])

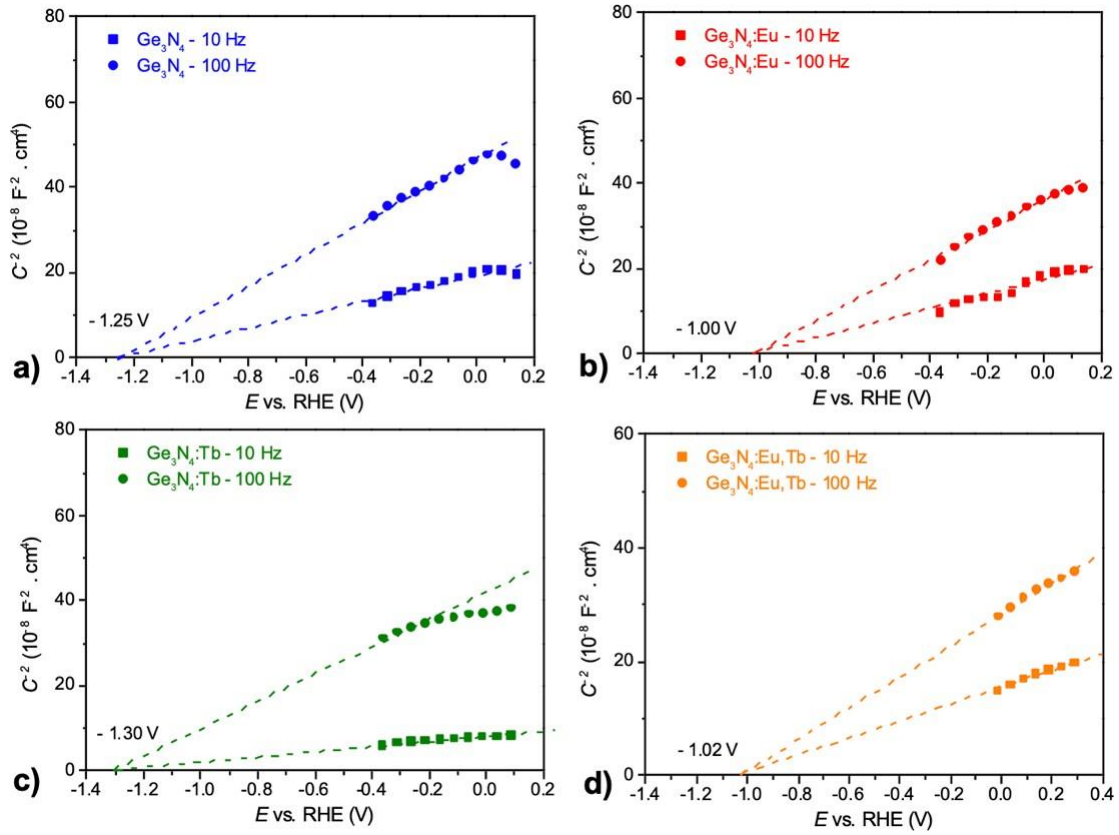


Figure S16: Mott-Schottky (MS) analysis of EIS measurements at an applied frequency of 10, 100 and 1000 Hz of a) pure $Ge_3N_4$ (blue), b) Tb-$Ge_3N_4$ (green), c) Eu-$Ge_3N_4$ (red) and d) Eu,Tb-$Ge_3N_4$:$Eu^{3+}$,$Tb^{3+}$ (orange). Measurements were performed in a 0.1 M potassium phosphate electrolyte in pH 7.

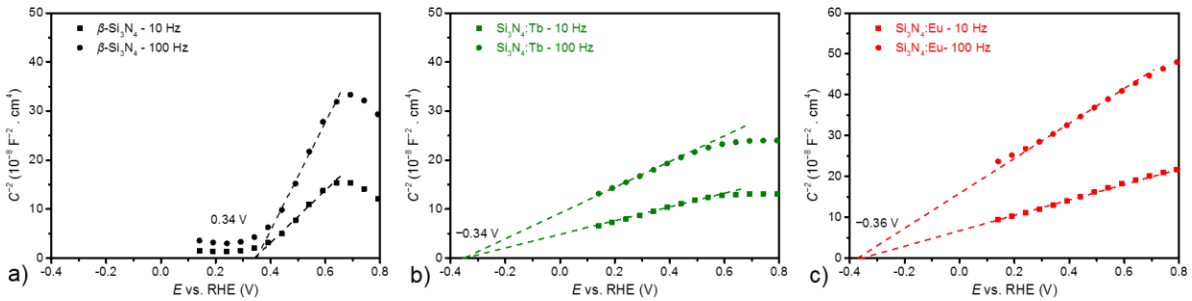


Figure S17: Mott-Schottky analysis of EIS measurements at an applied frequency of 10, and 100 Hz of a) undoped $Si_3N_4$ (black), b) Tb-$Si_3N_4$ (green) and c) Eu-$Si_3N_4$ (red). Measurements were performed in a 0.1 M potassium phosphate electrolyte in pH 7.

### *DFT calculations*

Calculations were carried out on pure and adsorbed β-$Si_3N_4$ and β-$Ge_3N_4$ within the Density Functional Theory (DFT) as implemented in the Vienna *ab initio* Simulation Package (VASP).[14–16] For electron exchange and correlation we used the Generalized Gradient approximation as parameterized by Perdew, Becke, and Ernzehof (PBE) functional.[17] Atom cores are described through the projector augmented wave (PAW) method.[18] The kinetic energy cutoff for plane wave expansions was set to 500 eV, and the Brillouin zone was sampled by Monkhorst–Pack meshes.[19] Atomic positions were optimized until forces were converged to lower than $3.10^{-2}$ eV/Å. DOS were shifted so that the Fermi level lies at 0 eV. For the geometry optimization the 4*f* states of the rare earths were placed in the pseudopotential, allowing to fix the oxidation degree to 3+ and to estimate the relative stabilities of both $Eu^{3+}$ and $Tb^{3+}$ in sites A and B. The calculations of the densities of states and magnetic properties was done by considering explicitly the 4*f* orbitals of the rare-earths in the valence states. Such an explicit treatment required to use GGA+U method[20] with a Hubbard term $U_{\text{eff}} = U - J = 6$ eV for the 4*f* (*RE*) states and to include the spin-orbit coupling (SOC).

### *References*


1 Y. Q. Li, N. Hirosaki, R. J. Xie, T. Takeda and M. Mitomo, *J. Lumin.*, 2010, **130**, 1147–1153.

2 M. Peres, K. Lorenz, E. Alves, E. Nogales, B. Méndez, X. Biquard, B. Daudin, E. G. Víllora and K. Shimamura, *J. Phys. D. Appl. Phys.*, 2017, **50**, 325101.

3 H. J. Lozykowski, W. M. Jadwisienczak, J. Han and I. G. Brown, *Appl. Phys. Lett.*, 2000, **77**, 767–769.

4 A. Nishikawa, T. Kawasaki, N. Furukawa, Y. Terai and Y. Fujiwara, *Appl. Phys. Express*, 2009, **2**, 071004.

5 Q. Li, C. Gong, X. Cheng and Y. Zhang, *Ceram. Int.*, 2015, **41**, 4227–4230.

6 L.-W. Yin, Y. Bando, Y.-C. Zhu and Y.-B. Li, *Appl. Phys. Lett.*, 2003, **83**, 3584–3586.

7 R. Su, Z. F. Huang, F. Chen, Q. Shen and L. M. Zhang, in *Key Engineering Materials*, Trans Tech Publications Ltd, 2017, vol. 727, pp. 635–641.

8 X. Xu, T. Nishimura, Q. Huang, R.-J. Xie, N. Hirosaki and H. Tanaka, *J. Am. Ceram. Soc.*, 2007, **90**, 4047–4049.

9 Z. Huang, F. Chen, Q. Shen and L. Zhang, *RSC Adv.*, 2016, **6**, 7568–7574.

10 Z. Huang, F. Chen, R. Su, Z. Wang, J. Li, Q. Shen and L. Zhang, *J. Alloys Compd.*, 2015, **637**, 376–381.

11 Z. Huang, R. Su, H. Yuan, J. Zhang, F. Chen, Q. Shen and L. Zhang, *Ceram. Int.*, 2018, **44**, 10858–10862.

12 Z. Huang, Z. Wang, H. Yuan, J. Zhang, F. Chen, Q. Shen and L. Zhang, *J. Mater. Sci.*, 2018, **53**, 13573–13583.

13 P. A. M. Berdowski, J. van Herk, L. Jansen and G. Blasse, *Phys. status solidi*, 1984, **125**, 387–391.

14 G. Kresse and J. Furthmüller, *Comput. Mater. Sci.*, 1996, **6**, 15–50.

15 G. Kresse and J. Hafner, *Phys. Rev. B*, 1994, **49**, 14251–14269.

16 G. Kresse and J. Furthmüller, *Phys. Rev. B*, 1996, **54**, 11169–11186.

17 J. P. Perdew, K. Burke and M. Ernzerhof, *Phys. Rev. Lett.*, 1997, **78**, 1396–1396.

18 P. E. Blöchl, *Phys. Rev. B*, 1994, **50**, 17953–17979.

19 H. J. Monkhorst and J. D. Pack, *Phys. Rev. B*, 1976, **13**, 5188–5192.

20 S. Dudarev and G. Botton, *Phys. Rev. B - Condens. Matter Mater. Phys.*, 1998, **57**, 1505–1509.